Reactivity of triruthenium thiophyne and furyne clusters: competitive S–C and P–C bond cleavage reactions and the generation of highly unsymmetrical alkyne ligands†

Md. Nazim Uddin,[a] Noorjahan Begum,[b] Mohammad R. Hassan,[a] Graeme Hogarth,*[c] Shariff E. Kabir,*[a] Md. Arzu Miah,[a] Ebbe Nordlander*[b] and Derek A. Tocher*[c]

Received 2nd May 2008, Accepted 1st September 2008
First published as an Advance Article on the web 30th September 2008
DOI: 10.1039/b806846a

The synthesis and reactivity of the thiophyne and furyne clusters $[Ru_3(CO)_7(\mu\text{-dppm})(\mu_3\text{-}\eta^2\text{-}C_4H_2E)\{\mu\text{-}P(C_4H_3E)_2\}(\mu\text{-}H)]$ (E = S, O) is reported. Addition of $P(C_4H_3E)_3$ to $[Ru_3(CO)_{10}(\mu\text{-dppm})]$ (**1**) at room temperature in the presence of Me_3NO gives simple substitution products $[Ru_3(CO)_9(\mu\text{-dppm})\{P(C_4H_3E)_3\}]$ (E = S, **2**; E = O, **3**). Mild thermolysis in the presence of further Me_3NO affords the thiophyne and furyne complexes $[Ru_3(CO)_7(\mu\text{-dppm})(\mu_3\text{-}\eta^2\text{-}C_4H_2E)\{\mu\text{-}P(C_4H_3E)_2\}(\mu\text{-}H)]$ (E = S, **4**; E = O, **6**) resulting from both carbon-hydrogen and carbon-phosphorus bond activation. In each the C_4H_2E (E = S, O) ligand donates 4-electrons to the cluster and the rings are tilted with respect to the μ-dppm and the phosphido-bridged open triruthenium unit. Heating **4** at 80 °C leads to the formation of the ring-opened cluster $[Ru_3(CO)_5(\mu\text{-}CO)(\mu\text{-dppm})(\mu_3\text{-}\eta^3\text{-}SC_4H_3)\{\mu\text{-}P(C_4H_3S)_2\}]$ (**5**) resulting from carbon-sulfur bond scission and carbon-hydrogen bond formation and containing a ring-opened $\mu_3\text{-}\eta^3$-1-thia-1,3-butadiene ligand. In contrast, a similar thermolysis of **3** affords the phosphinidene cluster $[Ru_3(CO)_7(\mu\text{-dppm})(\mu_3\text{-}\eta^2\text{-}C_4H_2O)\{\mu_3\text{-}P(C_4H_3O)\}]$ (**7**) resulting from a second phosphorus-carbon bond cleavage and (presumably) elimination of furan. Treatment of **4** and **6** with PPh_3 affords the simple phosphine-substituted products $[Ru_3(CO)_6(PPh_3)(\mu\text{-dppm})(\mu_3\text{-}\eta^2\text{-}C_4H_2E)\{\mu\text{-}P(C_4H_3E)_2\}(\mu\text{-}H)]$ (E = S, **8**; E = O, **9**). Both thiophyne and furyne clusters **4** and **6** readily react with hydrogen bromide to give $[Ru_3(CO)_6Br(\mu\text{-}Br)(\mu\text{-dppm})(\mu_3\text{-}\eta^2\text{-}\eta^1\text{-}C_4H_2E)\{\mu\text{-}P(C_4H_3E)_2\}(\mu\text{-}H)]$ (E = S, **10**; E = O, **11**) containing both terminal and bridging bromides. Here the alkynes bind in a highly unsymmetrical manner with one carbon acting as a bridging alkylidene and the second as a terminally bonded Fisher carbene. As far as we are aware, this binding mode has only previously been noted in ynamine complexes or those with metals in different oxidation states. The crystal structures of seven of these new triruthenium clusters have been carried out, allowing a detailed analysis of the relative orientations of coordinated ligands.

Introduction

The rearrangement of small organic molecules within the confines of low-valent transition metal clusters continues to be an active area of interest since it potentially allows insight into related transformations that may occur during heterogeneous catalytic processes. One particularly important illustration of this are attempts to model the key steps in the metal-catalysed hydrodesulfurisation of fossil fuels.[1–5] Thiophene is a key contaminant that needs to be removed and consequently its organometallic chemistry has been widely studied, but it does not generally act as a good ligand to low-valent metal clusters. Consequently, development of the organometallic chemistry of thiophene-derived ligands has been made using heterodifunctional phosphines such as diphenyl(2-thienyl)phosphine,[6–10] diphenyl(benzothienyl)phosphine,[10] di(2-thienyl)phenylphosphine,[10] and tri(2-thienyl)phosphine[10–14] which are capable of introducing the thienyl, C_4H_3S, ligand as a result of phosphorus-carbon bond cleavage.

The coordination chemistry of diphenyl(2-thienyl)phosphine has been especially well-developed.[6] For example, Deeming and co-workers have shown that it reacts with $Re_2(CO)_{10}$ to give $[Re_2(CO)_8(\mu\text{-}Ph_2PC_4H_3S)]$ (A, Chart 1) in which the intact ligand bridges the two metal atoms and this subsequently rearranges upon heating *via* phosphorus-carbon bond cleavage to give thienyl-bridged $[Re_2(CO)_8(\mu\text{-}PPh_2)(\mu\text{-}C_4H_3S)]$ (B). In contrast, the simple addition product of $Mn_2(CO)_{10}$ rearranges to afford $[Mn_2(CO)_6(\mu\text{-}PPh_2)(\mu\text{-}\eta^1\text{:}\eta^5\text{-}C_4H_3S)]$ in which the thienyl-bridge acts as a 7-electron donor (C).[6] Deeming also investigated the reaction of diphenyl(2-thienyl)phosphine with $Ru_3(CO)_{12}$;[7] here the major product is $[Ru_3(CO)_9(\mu_3\text{-}Ph_2PC_4H_2S)(\mu\text{-}H)]$ (D), containing a cyclometalated thienylphosphine ligand in which the sulfur remains non-metal bound.

We recently focused our attention towards developing the organometallic chemistry of tri(2-thienyl)phosphine and, by way of contrast, the related tri(2-furyl)phosphine.[15–16] These are

---

[a] *Department of Chemistry, Jahangirnagar University, Savar, Dhaka 1342, Bangladesh*
[b] *Inorganic Research Group, Chemical Physics, Center for Chemistry and Chemical Engineering, Lund University, P. O. Box 124, SE-22100 Lund, Sweden*
[c] *Department of Chemistry, University College London, 20 Gordon Street, London, UK WC1H OAJ*

† CCDC reference numbers 684188–684193 and 685951. For crystallographic data in CIF or other electronic format see DOI: 10.1039/b806846a

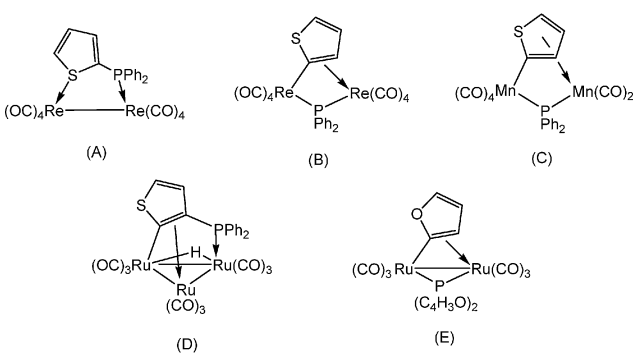

Chart 1

capable of delivering multiple thienyl and furyl rings respectively to cluster centres *via* phosphorus-carbon bond cleavage. Although tri(2-furyl)phosphine has become an important ligand in transition metal catalysis,[17] related studies with low-valent clusters remain virtually unexplored. Wong *et al.* have reported formation of binuclear $[Ru_2(CO)_6(\mu\text{-}C_4H_3O)\{\mu\text{-}P(C_4H_3O)_2\}]$ (E) from the reaction of $Ru_3(CO)_{12}$ with tri(2-furyl)phosphine at 67 °C resulting from carbon-phosphorus bond cleavage and coordination of the dissociated heteroaromatic group in a σ,π-alkenyl fashion.[18] Wong's group have also investigated the reaction of tri(2-furyl)phosphine with $[Ru_4(CO)_{12}(\mu\text{-}H)_4]$ obtaining a series of clusters containing furyl, furyne, phosphido- and phosphinidene ligands.[19] More recently, we reported the synthesis of di- and tri-substituted ruthenium clusters, $[Ru_3(CO)_{10}\{P(C_4H_3O)_3\}_2]$ and $[Ru_3(CO)_9\{P(C_4H_3O)_3\}_3]$, and their subsequent transformation under mild conditions to dinuclear (E) and $[Ru_2(CO)_5(\mu\text{-}C_4H_3O)\{\mu\text{-}P(C_4H_3O)_2\}\{P(C_4H_3O)_3\}]$ respectively *via* cleavage of metal-metal and phosphorus-carbon bonds.

Reactions of tri(2-thienyl)phosphine with $Os_3(CO)_{12}$ and $[(\mu\text{-}H)_2Os_3(CO)_{10}]$ leads to the formation of both simple substitution products as well as others resulting from cyclometalation,[13] related dirhodium cyclometalation complexes also being accessible.[11–12] In contrast, the only reported reactivity study of $Ru_3(CO)_{12}$ with tri(2-thienyl)phosphine lead to the isolation of low yields of $[Ru_3(CO)_{10}\{P(2\text{-}C_4H_3S)_3\}_2]$ and *trans*-$[Ru(CO)_3\{P(2\text{-}C_4H_3S)_3\}_2]$;[14] the latter being notable as it results from cluster fragmentation but contains intact tri(2-thienyl)phosphine ligands.

The work detailed above shows that reactions of both tri(2-thienyl)- and tri(2-furyl)phosphines with $Ru_3(CO)_{12}$ are characterized by cluster fragmentation. With this in mind, we turned our attention to the reactivity of both with the diphosphine-substituted triruthenium cluster $[Ru_3(CO)_{10}(\mu\text{-dppm})]$ (dppm = $Ph_2PCH_2PPh_2$).[20] This has been shown to exhibit significantly greater reactivity than the comparatively unreactive $Ru_3(CO)_{12}$,[21] while the small-bite angle diphosphine ligand is also highly effective at maintaining the integrity of the trinuclear cluster framework. Herein we describe reactions of $P(C_4H_3E)_3$ (E = O, S) with $[Ru_3(CO)_{10}(\mu\text{-dppm})]$ leading to the facile formation of trinuclear furyne- and thiophyne-hydride clusters the reactivity of which has been investigated. A key finding in the latter is the competitive nature of the activation of various E–C *versus* P–C bonds within these clusters and the selective formation of phosphinidene (E = O) and thia-1,3-butadiene (E = S) ligands, while in no instance is the well-known self-activation of the dppm ligand noted.[21–23] We also report the formation of complexes containing highly unsymmetrical alkyne ligands which we believe can be considered as binding in a terminal Fischer-carbene and bridging alkylidene fashion.

Results and discussion

(a) Carbonyl substitution products

Treatment of $[Ru_3(CO)_{10}(\mu\text{-dppm})]$ (**1**) with tri(2-thienyl)phosphine and tri(2-furyl)phosphine at room temperature in the presence of Me_3NO afforded $[Ru_3(CO)_9(\mu\text{-dppm})\{P(C_4H_3S)_3\}]$ (**2**) and $[Ru_3(CO)_9(\mu\text{-dppm})\{P(C_4H_3O)_3\}]$ (**3**) as red, air-stable crystalline solids in 90–95% yield (Scheme 1). Both have been fully characterized, **2** *via* a single-crystal X-ray diffraction analysis. The molecular structure is shown in Fig. 1 together with selected bond distances and angles and it is very similar to that of a number of related $[Ru_3(CO)_9(PR_3)(\mu\text{-dppm})]$ complexes.[24] All phosphorus atoms occupy equatorial sites and there are two short [Ru(1)–Ru(2) = 2.8523(3), Ru(2)–Ru(3) = 2.8622(3) Å] and one slightly longer [Ru(1)–Ru(3) = 2.8938(3) Å] ruthenium-ruthenium

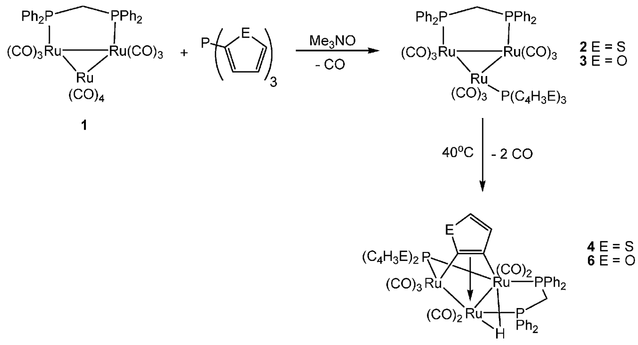

Scheme 1

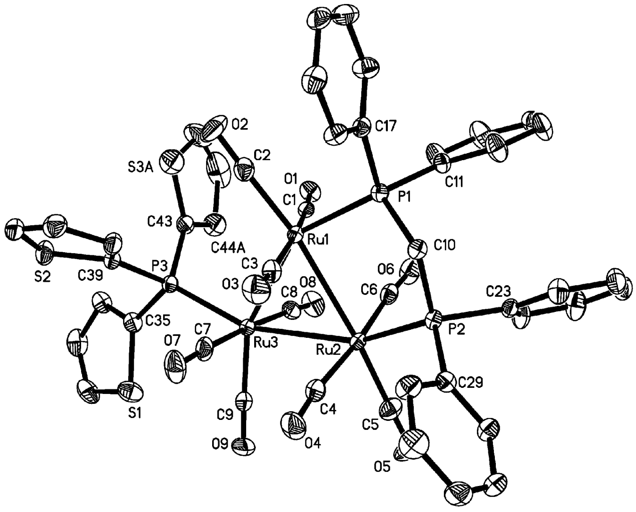

Fig. 1 Molecular structure of $[Ru_3(CO)_9(\mu\text{-dppm})\{P(C_4H_3S)_3\}]$ (**2**) with selected bond lengths (Å) and angles (°): Ru(1)–Ru(2) 2.8523(3), Ru(1)–Ru(3) 2.8938(3), Ru(2)–Ru(3) 2.8622(3), Ru(1)–P(1) 2.3366(8), Ru(2)–P(2) 2.3232(7), Ru(3)–P(3) 2.3374(8), Ru(2)–Ru(1)–Ru(3) 59.745(8), Ru(1)–Ru(2)–Ru(3) 60.847(8), Ru(2)–Ru(3)–Ru(1) 59.407(8), P(3)–Ru(3)–Ru(2) 159.88(2), P(3)–Ru(3)–Ru(1) 101.70(2), P(2)–Ru(2)–Ru(1) 94.01(2), P(2)–Ru(2)–Ru(3) 152.98(2), P(1)–Ru(1)–Ru(2) 88.91(2), P(1)–Ru(1)–Ru(3) 148.18(2), P(2)–C(10)–P(1) 111.50(14).

vectors. The latter lies opposite the monodentate phosphine [P(3)–Ru(3)–Ru(2) = 159.88(2)°] and the elongation results from the *trans*-influence of the former. The ruthenium-phosphorus bond distances [Ru(1)–P(1) = 2.3366(8), Ru(2)–P(2) = 2.3232(7) and Ru(3)–P(3) = 2.3374(8) Å] are comparable to those found in $[Ru_3(CO)_9(PR_3)(\mu\text{-dppm})]$ (R = Et, Ph, Cy, Pr^i) in which the phosphorus atoms are similarly bonded equatorially to the ruthenium triangle.[24]

Spectroscopic data are also similar to those reported for $[Ru_3(CO)_9(PR_3)(\mu\text{-dppm})]$.[24] The $^{31}P\{^1H\}$ NMR spectra of each displays two singlets (δ 16.4 and 1.9 for **2**; δ 16.4 and −14.3 for **3**) in an approximate 2:1 ratio showing that in solution the two ends of the dppm ligand are equivalent. This is attributed to the rapid fluxionality of $P(C_4H_3E)_3$ (E = S, O) between equatorial positions of the unique ruthenium atom and is similar to behavior noted in other complexes of this type. In adopting a terminal-equatorial coordination mode in **2–3**, $P(C_4H_3E)_3$ ligands serve as classic monodentate phosphorus-donors. This behavior is in contrast to the reactivity observed towards $Ru_3(CO)_{12}$[14,18] where in both cases monosubstituted clusters were not isolated presumably since they undergo further transformations under the reaction conditions used.

(b) Thiophyne and furyne complexes resulting from phosphorus-carbon and carbon-hydrogen bond cleavage

Heating either **2** or **3** at 40 °C in the presence of Me_3NO results in the clean formation of $[Ru_3(CO)_7(\mu\text{-dppm})(\mu_3\text{-}\eta^2\text{-}C_4H_2E)\{\mu\text{-}P(C_4H_3E)_2\}(\mu\text{-}H)]$ (E = S, **4**; E = O, **6**) (Scheme 1). Both have been fully characterized spectroscopically and by single crystal X-ray diffraction studies. The molecular structures of these isostructural clusters are depicted in Fig. 2 and 3 together with selected bond lengths and angles. Both contain an open triangular cluster of ruthenium atoms and seven terminal carbonyls. One edge is simultaneously bridged by the hydride (located and refined crystallographically) and the diphosphine and these metal-metal distances [Ru(1)–Ru(2) = 2.9406(3) Å in **4** and Ru(2)–Ru(3) = 2.9316(3) Å in **6**] are significantly longer than the non-hydride-bridged bonds [Ru(1)–Ru(3) = 2.8072(4) Å in **4** and 2.8182(4) Å in **6**] and also the corresponding dppm- and hydride-bridged metal-metal edge in $[Ru_3(CO)_6(\mu\text{-dppm})\{\mu_3\text{-}\eta^3\text{-}PhC{=}N(C_6H_4)PPh_2\}(\mu\text{-}H)]$ of 2.870(6) Å.[25] The open-edge of the ruthenium triangle [3.876 Å in **4** and 3.895 Å in **6**] is asymmetrically bridged by the new phosphido ligands and ruthenium-phosphorus bond distances and angles are similar to those found in other open triruthenium clusters[28–28] including $[Ru_3(CO)_5(\mu\text{-dppm})(\mu_3\text{-PPh})(\mu\text{-PPh}_2)_2]$.[26]

The most interesting features of these clusters are the coordination of μ_3-η^2-thiophyne and furyne ligands to the face of the cluster, formed by the cleavage of both carbon-phosphorus and carbon-hydrogen bonds. Both are slightly tilted on cluster surface towards the π-coordination side being similar to those previously observed for coordinated thiophyne in $[Os_3(CO)_9(\mu_3\text{-}\eta^3\text{-}SC_4H_2)(\mu\text{-}H)_2]$.[29] The C(35)–C(38) and C(10)–C(11) bonds in **4** and **6** of 1.427(4) and 1.416(4) Å respectively are typical of coordinated alkynes. The Ru–C π-bonding is quite symmetrical in **4** [Ru(1)–C(35) = 2.286(3) and Ru(1)–C(38) = 2.325(3) Å], but more asymmetric in **6** [Ru(3)–C(10) = 2.257(3) and Ru(3)–C(11) = 2.389(3) Å].

The mode of formation of **4** and **6** remains unknown and it is not clear whether carbon-hydrogen or carbon-phosphorus bond cleavage occurs initially. IR and TLC monitoring of the reactions gave no evidence of the presence of any intermediates. We speculate that hydride clusters, $[Ru_3(CO)_7(\mu\text{-dppm})\{\mu_3\text{-}(C_4H_2E)P(C_4H_3E)_2\}(\mu\text{-}H)]$ (E = S, O), resulting from cyclometalation of one a ring are initially formed since such products are the final products of the reaction of $Ph_2P(C_4H_3S)$ with $Ru_3(CO)_{12}$.[7] The absence of observable intermediates suggests that after the initial rate-determining cyclometalation, cleavage of the phosphorus-carbon bond is facile.

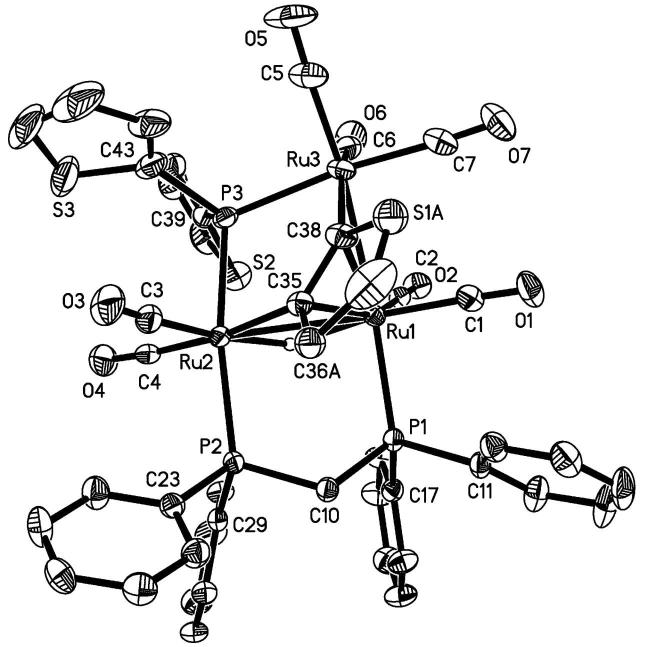

Fig. 2 Molecular structure of $[Ru_3(CO)_7(\mu\text{-dppm})(\mu_3\text{-}\eta^2\text{-}C_4H_2S)\{\mu\text{-}P(C_4H_3S)_2\}(\mu\text{-}H)]$ (**4**) with selected bond lengths (Å) and angles (°): Ru(1)–Ru(3) 2.8072(4), Ru(1)–Ru(2) 2.9406(3), Ru(1)–P(1) 2.3574(8), Ru(2)–P(2) 2.3687(8), Ru(2)–P(3) 2.3581(8), Ru(3)–P(3) 2.3862(8), Ru(1)–C(35) 2.286(3), Ru(1)–C(38) 2.325(3), Ru(2)–C(35) 2.123(3), Ru(3)–C(38) 2.104(3), Ru(3)–Ru(1)–Ru(2) 84.766(9), C(35)–Ru(1)–C(38) 36.04(10), C(35)–Ru(1)–Ru(3) 75.87(7), C(38)–Ru(1)–Ru(3) 47.26(8), C(35)–Ru(1)–Ru(2) 45.84(7), C(38)–Ru(1)–Ru(2) 72.68(8), C(38)–Ru(3)–Ru(1) 54.24(8), P(3)–Ru(2)–Ru(1) 78.373(19), P(3)–Ru(3)–Ru(1) 80.72(2), Ru(2)–P(3)–Ru(3) 109.55(3), C(38)–Ru(3)–P(3) 83.01(9), C(37)–S(1A)–C(38) 102.3(2), C(42)–S(2)–C(39) 92.25(18), C(43)–S(3)–C(46) 91.9(3), P(2)–C(10)–P(1) 111.85(14).

Both **4** and **6** exist as a mixture of two isomers in solution (Scheme 2) probably arising from the disposition of the bridging hydride ligand across the two inequivalent ruthenium-ruthenium edges. The hydride region of the ^1H NMR spectra are very similar and each contains two sets of signals in an approximate 10:1 ratio; a doublet of doublet of doublets (δ −14.95 for **4a** and −15.18 for **6a**) and a doublet of doublets (δ −14.93 for **4b** and −15.16 for **6b**). It seems reasonable to suggest that in the major isomer the hydride and dppm ligands bridge the same ruthenium-ruthenium edge as found in the solid-state, while in the minor isomer they span two different ruthenium-ruthenium edges. The aliphatic region of the spectra shows four sets of multiplets for the diastereotopic methylene protons and $^{31}P\{^1H\}$ NMR spectra exhibit two sets of three doublets of doublets (δ 32.5, 42.0 and 5.5 for **4a**; δ 39.7, 33.3 and 4.1 for **4b**; δ 42.8, 37.1 and −6.9 for **6a**; δ 39.8, 34.2 and −5.2 for **6b**) which are also attributed to the presence of two isomers.

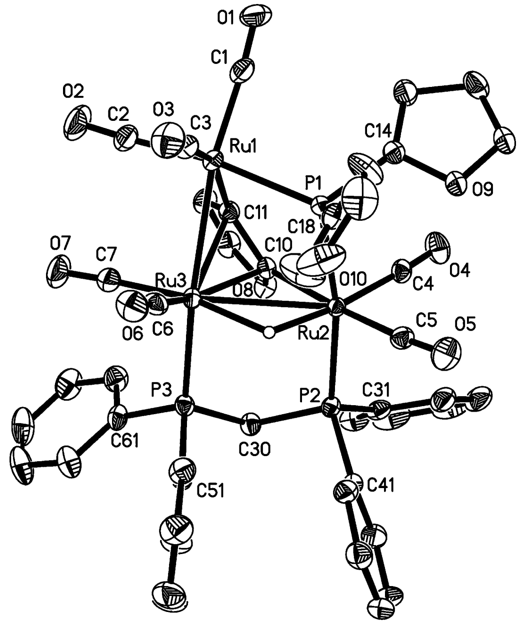

Fig. 3 Molecular structure of $[Ru_3(CO)_7(\mu\text{-dppm})(\mu_3\text{-}\eta^2\text{-}C_4H_2O)\{\mu\text{-}P(C_4H_3O)_2\}(\mu\text{-}H)]$ (**6**) with selected bond lengths (Å) and angles (°): Ru(1)–Ru(3) 2.8182(4), Ru(2)–Ru(3) 2.9316(3), Ru(1)–P(1) 2.3758(7), Ru(2)–P(1) 2.3554(7), Ru(2)–P(2) 2.3700(7), Ru(3)–P(3) 2.3542(8), C(10)–C(11) 1.416(4), Ru(1)–C(11) 2.089(3), Ru(2)–C(10) 2.094(3), Ru(3)–C(10) 2.257(3), Ru(3)–C(11) 2.389(3), C(10)–O(8) 1.417(3), C(14)–O(9) 1.382(4), C(18)–O(10) 1.337(4), Ru(1)–Ru(3)–Ru(2) 85.256(8), C(10)–Ru(3)–C(11) 35.34(9), C(11)–Ru(1)–Ru(3) 55.92(8), C(10)–Ru(2)–Ru(3) 50.04(7), C(10)–Ru(3)–Ru(1) 74.51(7), C(11)–Ru(3)–Ru(1) 46.40(7), P(1)–Ru(2)–Ru(3) 76.061(19), P(2)–Ru(2)–Ru(3) 93.429(19), P(3)–Ru(3)–Ru(1) 167.90(2), Ru(2)–P(1)–Ru(1) 110.82(3), C(13)–O(8)–C(10) 106.7(2), C(17)–O(9)–C(14) 107.1(2), C(18)–O(10)–C(21) 105.9(3), P(2)–C(30)–P(3) 113.34(15).

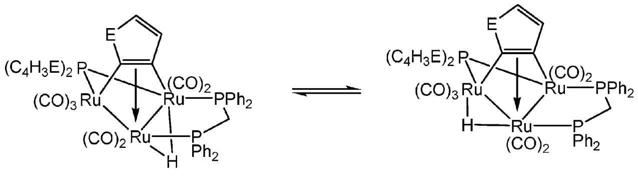

4a E = S
6a E = O

4b E = S
6b E = O

Scheme 2

(c) Sulfur-carbon bond cleavage: ring-opening of the thiophyne ligand

The importance of the enhanced reactivity of the phosphothiophene and phosphofuran ligands in **2** and **3** is further demonstrated by their thermal reactions at 80°C. Thermolysis of **2** in refluxing benzene provided, in addition to **4** (29%), the novel thiophyne ring-opened complex $[Ru_3(CO)_5(\mu\text{-}CO)(\mu\text{-dppm})(\mu_3\text{-}\eta^3\text{-}SC_4H_2)\{\mu\text{-}P(C_4H_3S)_2\}]$ (**5**) in 37% yield (Scheme 3). In a separate experiment, **4** converted into **5** in 68% yield after heating for 2.5 h in refluxing benzene. In contrast, a similar thermolysis of **3** afforded only **6** in 94% yield, and no evidence was obtained for the formation of a ring-opened product. Cluster **5** was characterized by a single-crystal X-ray diffraction analysis. The molecular structure is depicted in Fig. 4 together with selected bond lengths and angles, while Fig. 5 highlights the cluster core geometry.

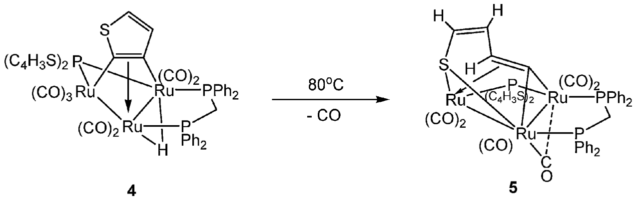

4 **5**

Scheme 3

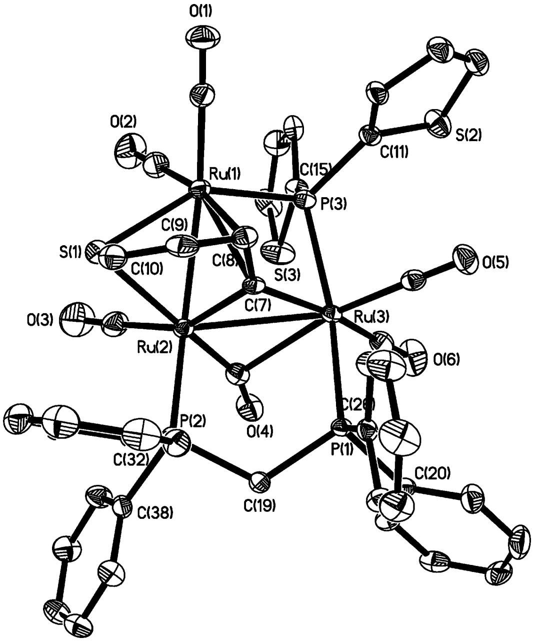

Fig. 4 Molecular structure of $[Ru_3(CO)_5(\mu\text{-}CO)(\mu\text{-dppm})(\mu_3\text{-}\eta^3\text{-}SC_4H_3)\{\mu\text{-}P(C_4H_3S)_2\}]$ (**5**) with selected bond lengths (Å) and angles (°): Ru(1)–Ru(2) 2.7030(8), Ru(2)–Ru(3) 2.8656(9), Ru(1)–P(3) 2.3254(11), Ru(2)–P(2) 2.3025(11), Ru(3)–P(3) 2.3949(11), Ru(3)–P(1) 2.4170(11), Ru(1)–S(1) 2.4001(11), Ru(2)–S(1) 2.4647(10), Ru(1)–C(7) 2.278(3), Ru(1)–C(8) 2.343(4), Ru(2)–C(7) 2.030(3), Ru(3)–C(7) 2.058(3), Ru(2)–C(4) 1.914(4), Ru(3)–C(4) 2.542(4), Ru(1)–Ru(2)–Ru(3) 77.689(11), C(7)–Ru(1)–C(8) 34.97(11), S(1)–Ru(1)–Ru(2) 57.39(3), C(7)–Ru(1)–Ru(2) 47.15(8), C(8)–Ru(1)–Ru(2) 76.11(9), P(2)–Ru(2)–Ru(1) 143.39(3), C(7)–Ru(2)–Ru(3) 45.88(9), S(1)–Ru(2)–Ru(3) 125.67(3), P(3)–Ru(3)–Ru(2) 83.37(3), Ru(1)–P(3)–Ru(3) 95.52(3), C(7)–Ru(2)–S(1) 82.84(10), S(1)–Ru(2)–Ru(1) 55.12(2), C(7)–Ru(3)–Ru(2) 45.10(9), Ru(1)–S(1)–Ru(2) 67.49(3), Ru(2)–C(4)–Ru(3) 78.67(12), C(8)–C(7)–Ru(3) 137.8(3), C(8)–C(7)–Ru(1) 75.1(2), Ru(3)–C(7)–Ru(1) 107.32(14), C(7)–C(8)–Ru(1) 69.96(19), P(2)–C(19)–P(1) 118.74(18).

The molecule represents a unique example of an open triruthenium cluster containing a capping 1-thia-1,3-butadiene ligand. This results from the cleavage of one carbon-sulfur bond of the coordinated thiophyne ligand and addition of the hydride to the cleaved ligand. The thiabutadiene bridges across the Ru(1)–Ru(2) edge through the sulfur atom [Ru(1)–S(1) = 2.4001(11), Ru(2)–S(1) = 2.4647(10) Å] and caps the ruthenium triangle through C(7) *via* Ru–C σ-bonds to two ruthenium atoms [Ru(3)–C(7) = 2.058(3) and Ru(2)–C(7) = 2.030(3) Å] and a π-bond to the third, Ru(1), through the atoms of formal carbon-carbon double bond, C(7)–C(8) of 1.390(5) Å [Ru(1)–C(7) = 2.278(3), Ru(1)–C(8) = 2.343(4) Å]. The other two carbon-carbon bond

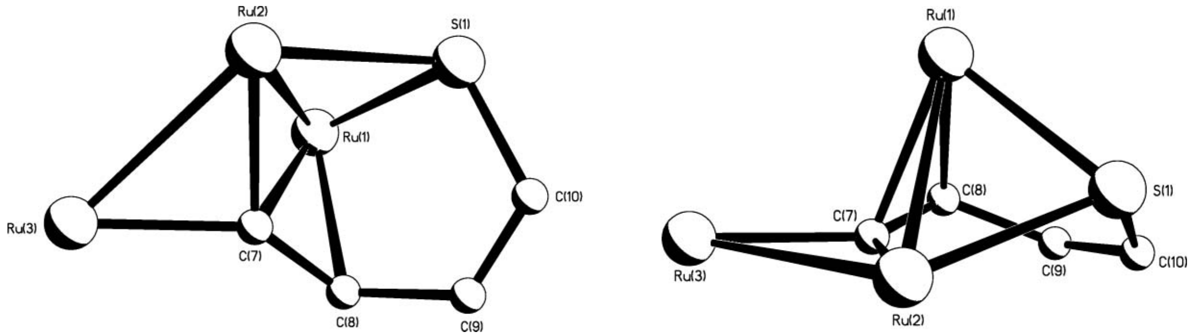

Fig. 5 Different views of the orientation of the 1-thia-1,3-butadiene ligand on the Ru_3 face of cluster **5**.

lengths [C(8)–C(9) = 1.479(5) and C(9)–C(10) = 1.321(6) Å] are clearly single and double bonds respectively and the diene is *cisoid* (Fig. 5). Together with the diphosphine and phosphido ligands, the remaining coordination sphere comprises five terminal and one semi-bridging carbonyl [Ru(2)–C(4) = 1.914(4), Ru(3)–C(4) = 2.542(4) Å]. The diphosphine occupies equatorial sites on Ru(2)–Ru(3) vector which is also bridged by C(7) of the 1-thia-1,3-butadiene ligand and the semi-bridging carbonyl. The open Ru(1)···Ru(3) edge of 3.495 Å is asymmetrically bridged [Ru(3)–P(3) = 2.3949(11) and Ru(3)–P(3) = 2.3254(11) Å] by the phosphido ligand with the diphosphine asymmetrically spanning the Ru(2)–Ru(3) edge [Ru(3)–P(1) = 2.4170(11) and Ru(2)–P(2) = 2.3025(11) Å], occupying equatorial coordination sites. Another noticeable feature of **5** is the expansion of the P–C–P bond angle by 6.89° as compared to **4**, possibly to accommodate the 1-thia-1,3-butadiene ligand. This expansion is also evident from the reduction of the Ru–Ru–Ru bond angle by 7.08° as compared to that in **4**.

Spectroscopic data for **5** are consistent with the solid-state structure. In addition to the resonances due to the diphosphine and phosphido ligands, the ^1H NMR spectrum contains two doublets at δ 6.67 ($J = 4.8$ Hz) and 3.89 ($J = 5.6$ Hz), and a doublet of doublets at δ 5.58 ($J = 5.6, 4.8$ Hz) assigned to the three protons of the 1-thia-1,3-butadiene ligand. The $^{31}P\{^1H\}$ NMR spectrum shows three doublet of doublets at δ 44.4 ($J = 238.3, 16.3$ Hz), 41.5 (dd, $J = 238.3, 75.5$ Hz) and –34.5 ($J = 75.5, 16.3$ Hz) consistent with the structure.

(d) Further phosphorus-carbon bond cleavage: Formation of a phosphinidene cluster

In order to compare the chemistry of the oxygen analogue **6** with that of **4**, we investigated the thermolysis of the former under more forcing conditions. Thus, refluxing a toluene solution of **6** yielded the new phosphinidene cluster $[Ru_3(CO)_7(\mu\text{-dppm})(\mu_3\text{-}\eta^2\text{-}C_4H_2O)\{\mu_3\text{-}P(C_4H_3O)\}]$ (**7**) in 70% yield (Scheme 4). This results from a second phosphorus-carbon bond activation of the bridging phosphido ligand, with concomitant loss of the hydride. These may be eliminated as furan, however, we have not shown this directly. Cluster **7** was fully characterized and a single-crystal X-ray diffraction analyses was also carried out, the results of which are summarised in Fig. 6 and its caption. The structure consists of an open arrangement of three ruthenium atoms with two metal-metal bonds [Ru(1)–Ru(2) = 2.8037(4) and Ru(1)–Ru(3) = 2.8648(4) Å] and a non-bonded separation [Ru(2)–Ru(3) = 4.038 Å]. The diphosphine spans the Ru(1)–Ru(3) edge which is marginally longer than the comparable edge in **1** [2.834(1) Å].[30] The furylphosphinidene ligand asymmetrically caps one side of the open ruthenium triangle; the two wingtips Ru–P distances [Ru(2)–P(3) = 2.3083(6) Å} and Ru(3)–P(3) = 2.2743(7) Å] being significantly shorter than the hinge Ru–P distance

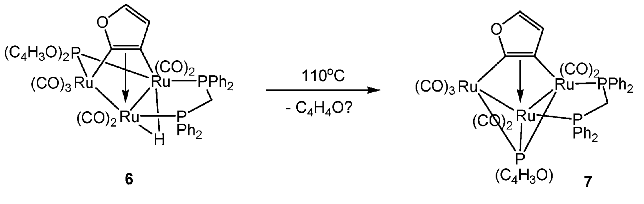

Scheme 4

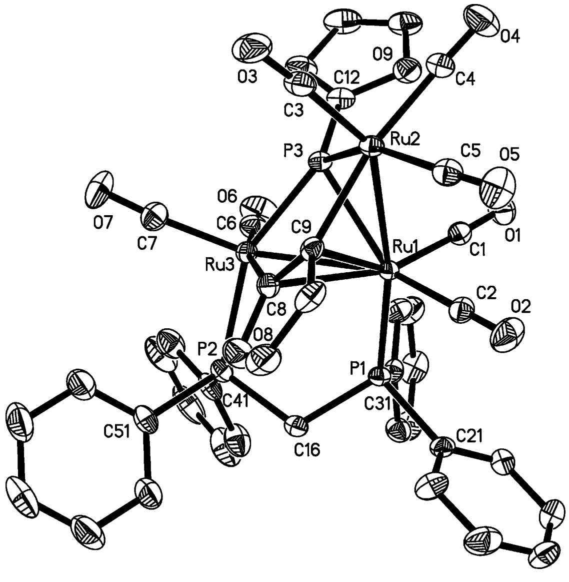

Fig. 6 Molecular structure of $[Ru_3(CO)_7(\mu\text{-dppm})(\mu_3\text{-}\eta^2\text{-}C_4H_2O)\{\mu_3\text{-}P(C_4H_3O)\}]$ (**7**) with selected bond lengths (Å) and angles (°): Ru(1)–Ru(2) 2.8037(4), Ru(1)–Ru(3) 2.8648(4), Ru(1)–P(1) 2.3224(7), Ru(1)–P(3) 2.4063(6), Ru(2)–P(3) 2.3083(6), Ru(3)–P(3) 2.2743(7), Ru(3)–P(2) 2.3718(7), Ru(1)–C(9) 2.384(2), Ru(1)–C(8) 2.389(2), Ru(2)–C(9) 2.085(2), Ru(3)–C(8) 2.091(2), Ru(2)–Ru(1)–Ru(3) 90.836(7), P(3)–Ru(1)–Ru(2) 51.916(16), P(3)–Ru(1)–Ru(3) 50.201(16), P(1)–Ru(1)–P(3) 127.81(2), P(1)–Ru(1)–Ru(3) 82.340(16), C(8)–Ru(1)–Ru(2) 74.57(6), C(8)–Ru(1)–Ru(3) 45.81(6), C(9)–Ru(1)–Ru(3) 74.02(6), C(9)–Ru(2)–Ru(1) 56.09(6), C(8)–Ru(3)–Ru(1) 55.00(6), C(9)–Ru(1)–C(8) 34.46(8), C(9)–Ru(1)–P(3) 71.78(6), C(8)–Ru(1)–P(3) 71.05(6), C(9)–Ru(2)–P(3) 79.30(7), P(2)–C(16)–P(1) 111.65(12).

[Ru(1)–P(3) = 2.4063(6) Å]. These ruthenium-phosphorus distances compare favorably with those found in other ruthenium clusters where a phosphinidene ligand caps an open triruthenium face (2.302–2.395 Å).[26–28] The μ_3-η^2-furyne ligand, which defines a six-vertex polyhedron containing a furylphosphinidene fragment occupying a basal vertex, caps the other face of the metal triangle through C(9) to Ru(1) and C(8) to Ru(3) and also being attached in a π-mode to C(9) and C(8). The Ru–C σ-bonding distances [Ru(2)–C(9) = 2.085(2), Ru(3)–C(8) = 2.091(2) Å] as well as the π-bonding distances [Ru(1)–C(9) = 2.384(2), Ru(1)–C(8) = 2.389(2) Å] are in good agreement with the corresponding distances in **6**. This type of coordination for the furylphosphinidene ligand has previously been observed in the tetraruthenium clusters $[Ru_4(CO)_{12-x}\{\mu_3\text{-}P(C_4H_3O)_2\}(\mu_3\text{-}\eta^2\text{-}C_4H_2O)(\mu\text{-}H)_2]$ (x = 0, 2, 3).[19]

Spectroscopic data are fully consistent with the solid-state structure. The $^{31}P\{^1H\}$ NMR spectrum contains three equal intensity doublet of doublets. The strongly deshielded signal at δ 328.0 (J = 185.2, 27.0 Hz) is assigned to the furylphosphinidene ligand and other signals at δ 28.5 (J = 69.6, 27.0 Hz) and 22.8 (J = 185.2, 69.6 Hz) to the diphosphine. In addition to the phenyl and methylene proton resonances of dppm ligand, the ^1H NMR spectrum contains five well-separated signals at δ 7.18, 7.01, 6.95, 6.66, 6.51 (each integrating for 1H) assigned to the protons of μ_3-η^2-C_4H_2O and μ_3-$P(C_4H_3O)$ ligands.

The selective cleavage of a phosphorus-carbon bond in **6** as compared to a sulfur-carbon bond scission seen in **4** is probably a consequence of the relative stability of the oxygen-carbon *versus* sulfur carbon bonds in these complexes. We note, however, that in previous studies by Deeming and co-workers,[7] heating cyclometalated $[Ru_3(CO)_9(\mu_3\text{-}Ph_2PC_4H_2S)(\mu\text{-}H)]$ with excess $Ru_3(CO)_{12}$ resulted in the formation of two tetranuclear phosphinidene-capped clusters, $[Ru_4(CO)_{11}(\mu_4\text{-}PPh)(\mu_4\text{-}C_6H_4)]$ and $[Ru_4(CO)_{11}(\mu_4\text{-}PPh)(\mu_4\text{-}C_4H_2S)]$. Here two carbon-phosphorus bonds are cleaved while the carbon-sulfur bond remains intact. Clearly this highlights the subtle factors affecting the relative rates of element-carbon bond cleavage in these closely related triruthenium clusters. A further point to note is that during all the thermal transformations of **4** and **6** no evidence was observed for any participation of the diphosphine ligand. This is somewhat surprising as facile carbon-hydrogen and carbon-phosphorus bond activation has been commonly observed for trinuclear dppm-bridged group 8 complexes.[21]

(e) Phosphine-substituted thiophyne and furyne clusters

Reactions of **4** and **6** with PPh_3 in refluxing benzene afforded the PPh_3 derivatives $[Ru_3(CO)_6(PPh_3)(\mu\text{-}dppm)(\mu_3\text{-}\eta^2\text{-}C_4H_2E)\{\mu\text{-}P(C_4H_3E)_2\}(\mu\text{-}H)]$ (E = S, **8**; E = O, **9**) in good yields (Scheme 5). Both were fully characterized and a single-crystal X-ray diffraction analysis was carried out for **9**. An ORTEP drawing of the molecular structure is depicted in Fig. 7 together with selected bond lengths and angles. It relates closely to **6** with the new phosphine occupying an equatorial site at the previously unsubstituted ruthenium centre. This lies effectively *cis* to the phosphido-bridge [P(3)–Ru(3)–P(4) 98.75(1)°] and *trans* to the Ru(2)–Ru(3) vector [P(3)–Ru(3)–Ru(2) 149.99(1)°]. The ruthenium-phosphorus distances involving the phosphido bridge [Ru(1)–P(4) = 2.369(2) Ru(3)–P(4) = 2.398(2) Å] are slightly longer than those observed in **6** as are the ruthenium-ruthenium distances [Ru(2)–Ru(3) = 2.9364(8), Ru(1)–Ru(3) = 2.8490(8) Å]. Other features of the two structures are very similar.

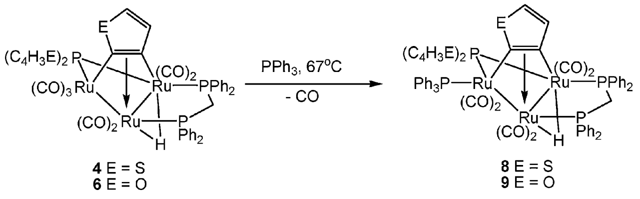

Scheme 5

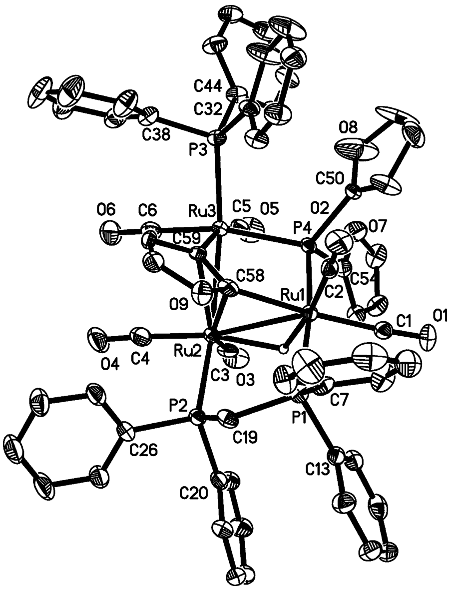

Fig. 7 Molecular structure of $[Ru_3(CO)_6(PPh_3)(\mu\text{-}dppm)(\mu_3\text{-}\eta^2\text{-}C_4H_2O)\{\mu\text{-}P(C_4H_3O)_2\}(\mu\text{-}H)]$ (**9**) with selected bond lengths (Å) and angles (°): Ru(1)–C(58) 2.120(8), Ru(1)–P(1) 2.3481(19), Ru(1)–P(4) 2.3694(19), Ru(1)–Ru(2) 2.9364(8), Ru(2)–C(58) 2.285(7), Ru(2)–C(59) 2.344(7), Ru(2)–P(2) 2.3713(19), Ru(2)–Ru(3) 2.8490(8), Ru(3)–C(59) 2.071(8), Ru(3)–P(3) 2.3472(19) Ru(3)–P(4) 2.3977(19), C(58)–Ru(1)–Ru(2) 50.64(19), P(1)–Ru(1)–Ru(2) 92.06(5), P(4)–Ru(1)–Ru(2) 77.27(5), C(58)–Ru(2)–Ru(1) 45.83(19), C(59)–Ru(2)–Ru(1) 72.65(17), P(2)–Ru(2)–Ru(1) 90.37(5), Ru(3)–Ru(2)–Ru(1) 84.41(2), C(58)–Ru(2)–C(59) 35.5(3), C(58)–Ru(2)–Ru(3) 73.87(19), C(59)–Ru(2)–Ru(3) 45.73(18), Ru(1)–P(4)–Ru(3) 109.26(7), P(1)–C(19)–P(2) 112.3(4).

Spectroscopic data for **8** and **9** indicate that they are isostructural. Pertinently, the closely related pattern of the carbonyl stretching frequencies in the IR spectra indicates that they have a similar distribution of carbonyls. Both exist as a mixture of two isomers in solution in approximately 10:1 ratio, which we attribute to different hydride locations. A similar finding was made for **4** and **6**. The $^{31}P\{^1H\}$ NMR spectra exhibit two sets of signals, each isomer having four overlapping doublet of doublet of doublets (δ 50.1, 40.8, 32.8 and 9.9 for **8a**; δ 47.5, 37.0 31.9 and 8.7 for **8b**; δ 50.3, 40.7, 35.8 and –0.1 for **9a**; δ 50.2, 38.1, 33.4 and –1.1 for **9b**) attributed to the four inequivalent phosphorus nuclei. Consistent with these observations, the methylene protons of the dppm ligand (δ 4.01 and 2.60 for **8a**, 3.51 and 2.80 for **8b**; δ 3.42 and 2.65 for **9a**, 3.20 and 2.76 for **9b**) and the bridging hydrides (δ –14.36 for **8a**; δ –14.55 for **8b** and δ –14.76 for **9a**; δ –15.0 for **9b**) each exhibit two sets of signals.

(f) Reactions of thiophyne and furyne clusters with HBr: synthesis of highly asymmetric alkyne complexes

Oxidative-addition of HBr to clusters often results in the net addition of 4-electrons with concomitant opening of two metal-metal bonds or loss of two carbonyls.[31] Bubbling HBr gas through thf solutions of **4** or **6** lead to an immediate color change and the isolation after chromatography of the new triruthenium clusters $[Ru_3(CO)_6Br(\mu\text{-}Br)(\mu\text{-}dppm)(\mu_3\text{-}\eta^2\text{-}\eta^1\text{-}C_4H_2E)\{\mu\text{-}P(C_4H_3E)_2\}(\mu\text{-}H)]$ (E = S, **10**; E = O, **11**) in moderate yields. Both were characterized by spectroscopic and analytical data but their precise nature only became clear from a single-crystal X-ray diffraction analysis of **11**. The molecular structure of **11** is depicted in Fig. 8 together with selected bond lengths and angles. The molecule consists of an open arrangement of ruthenium atoms with the expected bridging diphosphine, hydride and phosphido ligands together with one bridging and one terminal bromide. The hydride ligand was crystallographically located (refined) across the Ru(2)–Ru(3) edge, lying *trans* to carbonyl groups CO(3) and CO(5) and bent down towards the opposite face of the triangle occupied by the furyne. The Ru(2)–Ru(3) bond distance of 2.9379(5) Å is significantly shorter compared to the corresponding distances in **6**. The terminal bromide is equatorially coordinated [Ru(1)–Br(1) = 2.6197(6) Å]. The second bromide asymmetrically spans the open Ru(1)–Ru(3) edge [Ru(1)–Br(2) = 2.5588(6), Ru(3)–Br(2) = 2.6212(6) Å], while the phosphido ligand asymmetrically bridges the second open edge, namely Ru(1)–Ru(2) [Ru(1)–P(3) = 2.3098(12), Ru(2)–P(3) 2.3815(12) Å].

Perhaps the most striking feature of **11** is the nature of the furyne ligand which is now quite different to that found in **6**. While it still spans all three ruthenium atoms so as to cap one face of the triruthenium core it binds very asymmetrically lying approximately perpendicular to the ruthenium-ruthenium bonded edge (Fig. 9). One of the carbons, C(10), bridges this edge slightly asymmetrically [Ru(2)–C(10) = 2.196(4) and Ru(3)–C(10) = 2.148(4) Å]. This is bound to a further carbon, C(11), the carbon-carbon bond length of 1.435(6) Å is significantly greater than that found in **6** (1.416(4) Å) and other alkyne complexes described in this paper. This second carbon is now bound to a single metal atom. The Ru(1)–C(11) bond distance of 2.079(4) Å is similar to the ruthenium-carbon σ bond distances in **6** while distances of 3.009 and 3.178 Å to Ru(2) and Ru(3) respectively are clearly non-bonding. The furyne ring has clear double and single bond character as shown by the C(11)–C(12) and C(12)–C(13) distances of 1.413(6) and 1.353(6) Å.

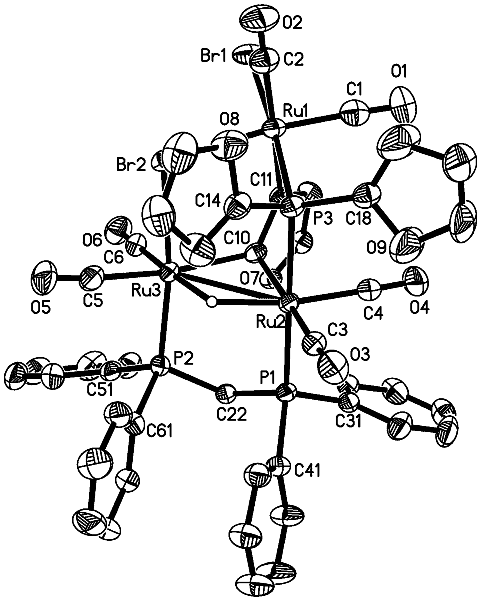

Fig. 8 Molecular structure of $[Ru_3(CO)_6Br(\mu\text{-}Br)(\mu\text{-}dppm)(\mu_3\text{-}\eta^2\text{-}\eta^1\text{-}C_4H_2O)\{\mu\text{-}P(C_4H_3O)_2\}(\mu\text{-}H)]$ (**11**) with selected bond lengths (Å) and angles (°): Ru(1)–C(11) 2.079(4), Ru(1)–P(3) 2.3098(12), Ru(1)–Br(2) 2.5588(6), Ru(1)–Br(1) 2.6197(6), Ru(2)–C(10) 2.196(4), Ru(2)–P(3) 2.3815(12), Ru(2)–P(1) 2.4082(12), Ru(2)–Ru(3) 2.9379(5), Ru(3)–C(10) 2.148(4), Ru(3)–P(2) 2.2859(12), Ru(3)–Br(2) 2.6212(6), Br(2)–Ru(1)–Br(1) 91.77(2), P(3)–Ru(1)–Br(2) 84.51(3), P(3)–Ru(1)–Br(1) 173.64(3), P(3)–Ru(2)–P(1) 177.60(4), P(3)–Ru(2)–Ru(3) 88.58(3), P(1)–Ru(2)–Ru(3) 90.69(3), Br(2)–Ru(3)–Ru(2) 98.243(17), Ru(1)–Br(2)–Ru(3) 102.127(19), Ru(1)–P(3)–Ru(2) 112.14(5), C(10)–Ru(2)–Ru(3) 46.77(11), C(10)–Ru(3)–Ru(2) 48.14(12), Ru(3)–C(10)–Ru(2) 85.10(15), P(2)–C(22)–P(1) 110.1(2).

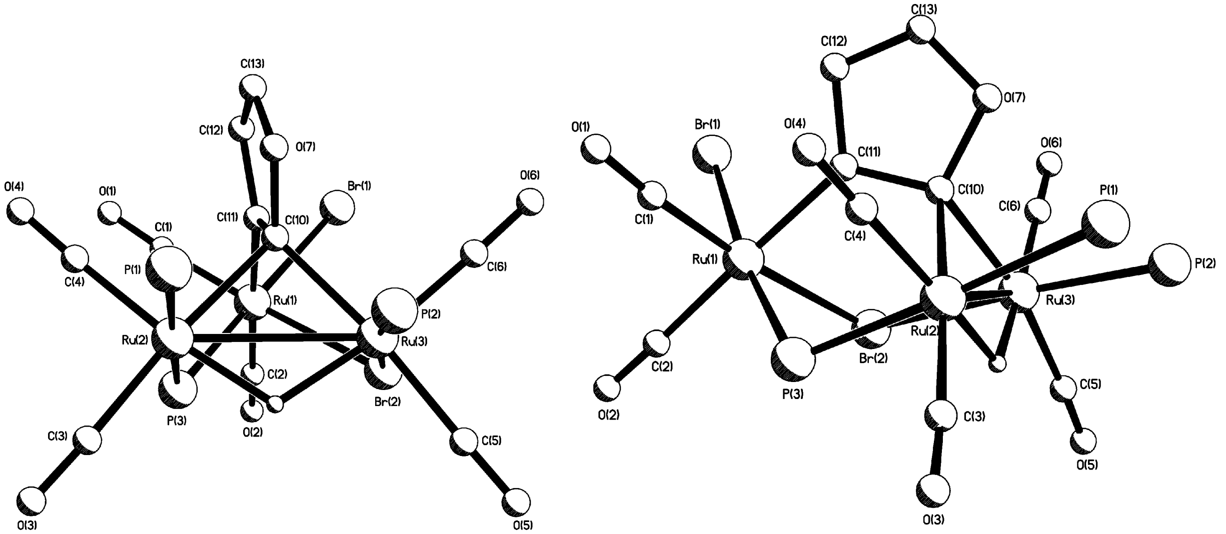

Fig. 9 Two views of the central core of **11** highlighting the relative positions of furyne and ruthenium atoms and the octahedral nature of Ru(1).

In light of these metric parameters, we favour the coordination mode shown in Scheme 6 for the furyne binding in **11**. Hence, the ligand can be considered as a hybrid bridging-terminal carbene; one carbon binding to a ruthenium atom in a terminal fashion while the second bridges a ruthenium-ruthenium bond. While the binding of alkynes to low-valent clusters is well-documented[32] as far as we are aware this type of alkyne binding is extremely rare and has previously been confined to heterobimetallic complexes containing metals in significantly different oxidation states,[33] or ynamine complexes.[34–38] The alkyne binding in **11** most closely resembles that in $[Os_3(CO)_9(\mu\text{-}H)_2\{\mu_3\text{-}\eta^2\text{-}\eta^1\text{-}HC\text{–}C(NEt_2)\}]$ (F) which can be prepared from the reaction of $[Os_3(CO)_9(\mu\text{-}H)(\mu_3\text{-}\eta^2\text{-}\eta^1\text{-}C_2H)]$ with diethylamine,[38] or upon heating the alkylidyne complex $[Os_3(CO)_9(\mu\text{-}H)_2\{\mu_3\text{-}\eta^1\text{-}C\text{-}CH(=NEt_2)\}]$.[37] Adams and Tanner formulated the ynamine ligand in **F** as a combination of terminal and bridging carbene ligands and our current data concur with this approach. It is noteworthy that in **F** and other ynamine complexes, the amine group is bound to the terminally bonded carbon, however in both **10–11** the electronegative heteroatom is bound to the bridging carbene carbon.

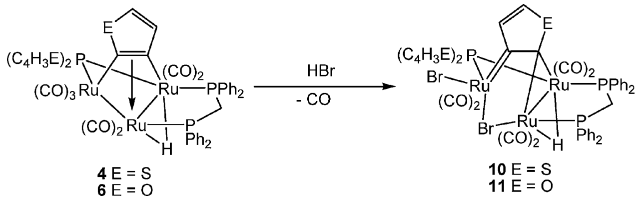

Scheme 6

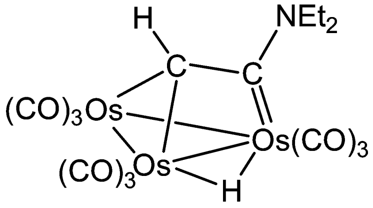

(F)

The coordination geometry of Ru(1) is octahedral with *cis*-carbonyls and *cis*-bromides, one carbonyl lying *trans* to C(11) and the terminal bromide lying *trans* to the phosphido-bridge. Ruthenium-carbon bonds in terminal alkylidene complexes tend to be of the order 1.85–1.90 Å,[39] but these are commonly five-coordinate and cannot be directly compared to **6**. With this model in mind, we also note the significant elongation of the carbonyl *trans* to C(11) [Ru(1)–C(2) 1.960(5) Å] as compared to that *trans* to the bridging bromide [Ru(1)–C(1) 1.858(6) Å], and that the terminal bromide distance [Ru(1)–Br(1) = 2.6197(6) Å] is *longer* than that to the bridging bromide [Ru(1)–Br(2) = 2.5588(6) Å].

The spectroscopic data of **11** indicate that its solid-state structure is maintained in solution and data for **10** indicate that it is isostructural. The $^{31}P\{^1H\}$NMR spectra exhibit two doublets [δ 48.4 (J = 70.4 Hz), −9.8 (J = 91.6 Hz for **10**; δ 48.3 (J = 64.4 Hz), −10.10 (J = 85.6 Hz) for **11**] and a doublet of doublets [δ 21.7 (J = 70.4, 91.6 Hz) for **10**; δ 22.1 (J = 64.4, 85.6 Hz) for **11**] consistent with their solid-state structures. The hydride region of the ^{1}H NMR spectra of both contains an overlapping doublet of doublets (δ −11.87 for **10**; −11.85 for **11**) and their mass spectra confirm the stoichiometry with molecular ion peaks being observed in each case (*m*/*z* 1297 for **10** and 1249 for **11**). Unfortunately due to the relatively small amounts of **10** and **11** we have been unable to acquire high quality ^{13}C NMR data in order to establish the electronic characteristics of the carbon atoms of the alkyne ligand.

Conclusions

This paper demonstrates that both tri(2-furyl)phosphine and tri(2-thienyl)phosphine are versatile synthons for a series of new triruthenium clusters. The transformation of **2** into **4** and **5** represents a previously unprecedented cluster-promoted sequential activation of carbon-hydrogen, carbon-phosphorus and carbon-sulfur bonds of coordinated tri(2-thienyl)phosphine ligand leading to a ring-opened μ_3-η^3-1-thia-1,3-butadiene ligand. In contrast, while the transformation of **3** into **6** follows similar phosphorus-carbon and carbon-hydrogen bond activation processes, ring-opening of the coordinated furyne ligand in **6** does not occur under more forcing conditions. Rather the phosphinidene cluster **7** results from a further carbon-phosphorus bond activation of the bridging phosphido ligand. This difference in reactivity can be rationalised in terms of the strong carbon-oxygen *versus* carbon-sulfur bond.

Addition of hydrogen bromide to both thiophyne and furyne clusters results in the formation of new alkyne clusters in which the hydrocarbon ligand binds highly asymmetrically to the three metal atoms. We favour a bonding picture in which the terminally bonded carbon acts like a Fischer-carbene and the second carbon a bridging alkylidene. This then suggests that the carbon-carbon interaction is best described as a single bond. We are still developing this bonding picture using DFT calculations[40] and hope to report the details of these in the near future. The synthesis of **10** and **11** opens up the possibility of exploring the chemistry of these interesting compounds, and work in this direction is currently underway in our laboratories. In this context we note that there are a small number of examples of related osmium clusters bearing terminally bonded carbene ligands[41,42] and these have been shown to display high reactivity.[43–46] We are currently investigating the reactivity of **10** and **11** and will report on these in the near future.

Experimental

Methods and materials

All reactions were performed under a nitrogen atmosphere. Reagent grade solvents were dried by the standard procedures and were freshly distilled prior to use. $[Ru_3(CO)_{10}(\mu\text{-dppm})]$ (**1**) was prepared according to the literature.[47] Tri(2-thienyl)phosphine and tri(2-furyl)phosphine were purchased from Across and used as received. Preparative thin-layer (TLC) plates were prepared from silica gel (Kieselgel DGF$_{254}$). Infrared spectra were recorded on a Shimadzu FTIR 8101 spectrophotometer. NMR spectra were recorded on Varian Unity Plus 500 and Bruker DPX 400 instruments. The chemical shifts were referenced to residual solvent resonances or external 85% H_3PO_4 in ^{1}H and ^{31}P NMR spectra as appropriate. Elemental analyses were performed by Microanalytical Laboratories, University College London. Fast atom bombardment mass spectra were obtained on a JEOL SX-102 spectrometer using 3-nitrobenzyl alcohol as matrix and CsI as calibrant.

Syntheses

[Ru$_3$(CO)$_9$(μ-dppm){P(C$_4$H$_3$S)$_3$}] (2). To a dichloromethane solution (30 cm^3) of [Ru$_3$(CO)$_{10}$(μ-dppm)] (**1**) (100 mg, 0.103 mmol) and P(C$_4$H$_3$S)$_3$ (36 mg, 0.128 mmol) was added dropwise a dichloromethane solution (15 cm^3) of Me$_3$NO (8 mg, 0.103 mmol). The reaction mixture was stirred at room temperature for 1.5 h during which time the color changed from orange to red. The solution was filtered through a short silica column (2 cm) and the solvent from the filtrate was removed under reduced pressure. The residue was recrystallised from hexane/CH$_2$Cl$_2$ at 4 °C to give [Ru$_3$(CO)$_9$(μ-dppm){P(C$_4$H$_3$S)$_3$}] (**2**) (113 mg, 90%) as red crystals. Calc. for C$_{46}$H$_{31}$O$_9$P$_3$Ru$_3$S$_3$: C, 45.28; H, 2.56. Found: C, 45.51; H, 2.65%. IR (*v*CO, CsH$_2$Cl$_2$) 2055 w, 1995 *vs*, 1979 *vs*, 1945 m cm^{-1}. ^{1}H NMR (CDCl$_3$): δ 7.53 (m, 3H), 7.50 (m, 3H), 7.33 (m, 20H), 7.12 (m, 3H), 4.20 (t, *J* = 10.4 Hz, 3H). ^{31}P{^{1}H} NMR (CDCl$_3$): δ 16.4 (s, 2P), 1.9 (s, 1P). FAB MS: *m/z* 1221 (M$^+$).

[Ru$_3$(CO)$_9$(μ-dppm){P(C$_4$H$_3$O)$_3$}] (3). A similar reaction to that above using **1** (100 mg, 0.103 mmol), P(C$_4$H$_3$O)$_3$ (30 mg, 0.128 Me$_3$NO (8 mg, 0.103 mmol) afforded [Ru$_3$(CO)$_9$(μ-dppm){P(C$_4$H$_3$O)$_3$}] (**3**) (115 mg, 95%) as red crystals. Calc. for C$_{46}$H$_{31}$O$_{12}$P$_3$Ru$_3$: C, 47.15; H, 2.67. Found: C, 47.38; H, 2.90%. IR (*v*CO, CH$_2$Cl$_2$) 2057 w, 1996 *vs*, 1981 *vs*, 1943 m cm^{-1}. ^{1}H NMR (CDCl$_3$): δ 7.65 (s, 3H), 7.34 (m, 20H), 6.70 (m, 3H), 6.43 (m, 3H), 4.21 (t, *J* = 10.2 Hz, 3H). ^{31}P{^{1}H} NMR (CDCl$_3$): δ 16.4 (s, 2P), −14.3 (s, 1P). FAB MS: *m/z* 1173 (M$^+$).

[Ru$_3$(CO)$_7$(μ-dppm)(μ$_3$-η^2-C$_4$H$_2$S){μ-P(C$_4$H$_3$S)$_2$}(μ-H)] (4). A dichloromethane solution (30 cm^3) of **2** (100 mg, 0.082 mmol) and Me$_3$NO (20 mg, 0.267 mmol) was refluxed 40 h during which time the color changed from red to yellow. The solvent was removed under reduced pressure and the residue chromatographed by TLC on silica gel. Elution with hexane/CH$_2$Cl$_2$ (3:2, v/v) developed two bands. The first band gave [Ru$_3$(CO)$_7$(μ-dppm)(μ$_3$-η^2-C$_4$H$_2$S){μ-P(C$_4$H$_3$S)$_2$}(μ-H)] (**4**) (55 mg, 60%) as pale yellow crystals after recrystallisation from CH$_2$Cl$_2$/hexane at 4 °C. Calc. for C$_{43}$H$_{31}$O$_7$P$_3$Ru$_3$S$_3$: C, 44.83; H, 2.71. Found: C, 44.98; H, 2.84. IR (*v*CO, CH$_2$Cl$_2$): 2057 *vs*, 2036 *vs*, 2000 *vs*, 1991 *vs*, 1943 w cm^{-1}. ^{1}H NMR (CDCl$_3$): major isomer (**4a**), δ 7.82 (d, *J* = 4.0 Hz, 1H), 7.69 (m, 4H), 7.50 (m, 6H), 7.34 (m, 2H), 7.20 (m, 3H), 7.13 (m, 5H), 7.00 (m, 2H), 6.87 (m, 2H), 6.82 (d, *J* = 4.0 Hz, 1H), 6.48 (m, 2H), 3.77 (m, 1H), 2.77 (m, 1H) −14.95 (ddd, *J* = 16.0, 10.2, 8.0 Hz, 1H). ^{31}P{^{1}H} NMR (CDCl$_3$): δ 42.0 (dd, *J* = 224.9, 8.9 Hz, 1P), 33.2 (dd, *J* = 76.8, 8.9 Hz, 1P), 5.5 (dd, *J* = 224.9, 76.8 Hz, 1P); minor isomer (**4b**), δ 7.78 (d, *J* = 4.0 Hz, 1H), 7.65 (m, 4H), 7.45 (m, 6H), 7.31 (m, 2H), 7.18 (m, 3H), 7.12 (m, 5H), 6.96 (m, 2H) 6.84 (m, 2H), 6.79 (d, *J* = 4.0 Hz, 1H), 6.41 (m, 2H), 2.89 (m, 1H), 2.56 (m, 1H), −14.93 (dd, *J* = 16.4, 16.0 Hz, 1H). ^{31}P{^{1}H} NMR (CDCl$_3$): δ 39.7 (dd, *J* = 230.2, 8.2 Hz, 1P), 32.5 (dd, *J* = 86.4, 8.2 Hz, 1P), 4.1 (dd, *J* = 230.2, 86.4 Hz, 1P) **4b**. The second band gave unconsumed **2** (4 mg). FAB MS: *m/z* 1153 (M$^+$).

[Ru$_3$(CO)$_5$-(μ-CO)(μ-dppm)(μ$_3$-η^3-SC$_4$H$_3$){μ-P(C$_4$H$_3$S)$_2$}] (5). A benzene solution (30 cm^3) of **2** (100 mg, 0.082 mmol) was heated to reflux for 3.5 h during which time the colour changed from red to deep red. The solvent was removed under reduced pressure and the residue chromatographed by TLC on silica gel. Elution with hexane/CH$_2$Cl$_2$ (6:4, v/v) developed two bands. The first band gave **4** (27 mg, 29%) while the band [Ru$_3$(CO)$_5$(μ-CO)(μ-dppm)(μ$_3$-η^3-SC$_4$H$_3$){μ-P(C$_4$H$_3$S)$_2$}] (**5**) (35 mg, 37%) as red crystals after recrystallisation from CH$_2$Cl$_2$/hexane at 4 °C. Likewise, refluxing a benzene solution (20 mL) of **4** (30 mg, 0.026 mmol) for 2.5 h yielded **5** (20 mg, 68%) and some unconverted starting material (7 mg, 23%). Calc. for C$_{43}$H$_{31}$O$_6$P$_3$Ru$_3$S$_3$: C, 45.46; H, 2.75. Found: C, 45.72; H, 2.93%. IR (*v*CO, CH$_2$Cl$_2$): 2029 s, 2006 *vs*, 1983 *vs*, 1943 s, 1844 w cm^{-1}. ^{1}H NMR (CDCl$_3$): δ 7.62 (m, 2H), 7.44 (m, 8H), 7.29 (s, 3H), 7.14 (m, 13H), 6.67 (d, *J* = 4.8 Hz, 1H), 5.58 (dd, *J* = 5.6, 4.8 Hz, 1H) 3.89 (d, *J* = 5.6 Hz, 1H), 2.83 (m, 1H), 2.20 (m, 1H). ^{31}P{^{1}H} NMR (CDCl$_3$): δ 44.4 (dd, *J* = 238.1, 16.3 Hz,1P), 41.5 (dd, *J* = 75.5, 238.1 Hz 1P), −34.5 (dd, *J* = 75.5, 16.3 Hz, 1P). FAB MS: *m/z* 1137 (M$^+$).

[Ru$_3$(CO)$_7$(μ-dppm)(μ$_3$-η^2-C$_4$H$_2$O){μ-P(C$_4$H$_3$O)$_2$}(μ-H)] (6). A dichloromethane solution (40 cm^3) of [Ru$_3$(CO)$_9$(μ-dppm){P(C$_4$H$_3$O)$_3$}] (**3**) (100 mg, 0.085 mmol) and Me$_3$NO (21 mg, 0.28 mmol) was refluxed for 34 h during which time the colour changed from red to yellow. Analytical TLC indicated complete conversion to a new product. The solvent was removed *in vacuo* and the residue washed with cold acetone to give [Ru$_3$(CO)$_7$(μ-dppm)(μ$_3$-η^2-C$_4$H$_2$O){μ-P(C$_4$H$_3$O)$_2$}(μ-H)] (**6**) (88 mg, 94%) as yellow crystals after recrystallisation from hexane/CH$_2$Cl$_2$ at 4°C. A similar thermolysis of [Ru$_3$(CO)$_9$(μ-dppm){P(C$_4$H$_3$O)$_3$}] (**2**) (100 mg, 0.085 mmol) in refluxing benzene (30 mL) for 1 h followed by similar work up afforded **6** in high yield. Calc. for C$_{43}$H$_{31}$O$_{10}$P$_3$Ru$_3$: C, 46.79; H, 2.83. Found: C, 46.98; H, 2.96%. IR (*v*CO, CH$_2$Cl$_2$): 2058 *vs*, 2038 *vs*, 2000 *vs*, 1993 *vs*, 1947 w cm^{-1}. ^{1}H NMR (CDCl$_3$): major isomer (**6a**), δ 7.83 (m, 1H), 7.70 (m, 4H), 7.45 (m, 6H), 7.19 (m, 8H), 6.97 (m, 3H), 6.60 (m, 3H), 6.36 (m, 2H), 6.24 (m, 1H), 3.25 (m, 1H), 2.64 (m, 1H), −15.18 (ddd, *J* = 11.2, 6.0 Hz, 1H). ^{31}P{^{1}H} NMR (CDCl$_3$): δ 42.8 (dd, *J* = 216.0, 122.0 Hz, 1P), 37.1 (dd, *J* = 122.0, 17.0 Hz, 1P), −6.9 (dd, *J* = 216.0, 17.0 Hz, 1P); minor isomer (**6b**), δ 7.78 (m, 1H), 7.71 (m, 4H), 7.54 (m, 6H), 7.14 (m, 8H), 7.02 (m, 3H), 7.90 (m, 3H), 6.80 (m, 2H), 6.25 (m, 1H), 3.04 (m, 1H), 2.74 (m, 1H), −15.16 (dd, *J* = 16.0, 17.2 Hz, 1H). ^{31}P{^{1}H} NMR (CDCl$_3$): δ 39.8 (dd, *J* = 216.2, 104.7 Hz, 1P), 34.2 (dd, *J* = 104.7, 18.8 Hz, 1P), −5.2 (dd, *J* = 216.2, 18.8 Hz, 1P). FAB MS: *m/z* 1105 (M$^+$).

[Ru$_3$(CO)$_7$(μ-dppm)(μ$_3$-η^2-C$_4$H$_2$O){μ$_3$-P(C$_4$H$_3$O)}] (7). A solution of **6** (30 mg, 0.027 mmol) in toluene (25 mL) was refluxed for 4.5 h. A similar chromatographic separation to that above afforded **6** (5 mg) and [Ru$_3$(CO)$_7$(μ-dppm)(μ$_3$-η^2-C$_4$H$_2$O){μ$_3$-P(C$_4$H$_3$O)}] (**7**) as yellow crystals (20 mg, 70%) after recrystallisation from hexane/CHCl$_3$ at 4 °C. Calc. for C$_{40}$H$_{27}$O$_9$P$_3$Ru$_3$: C, 45.85; H, 2.60. Found: C, 46.05; H, 2.81. IR (*v*CO, CH$_2$Cl$_2$) 2062 *vs*, 2009 *vs*, 1995 s, 1975 s, 1958 s cm^{-1}. ^{1}H NMR (CDCl$_3$): δ 7.70 (m, 5H), 7.39 (m, 5H), 7.28 (m, 5H), 7.18 (d, *J* = 2.0 Hz, 1H), 7.13 (m, 5H), 7.01 (d, *J* = 1.5, 1H), 6.95 (d, *J* = 2.0 Hz, 1H), 6.66 (d, *J* = 2.0 Hz, 1H), 6.51 (dd, *J* = 1.5, 2.0 Hz, 1H), 4.20 (m, 2H). ^{31}P{^{1}H} NMR (CDCl$_3$): δ 328.0 (dd, *J* = 185.2, 27.0 Hz, 1P), 28.5 (dd, *J* = 69.6, 27.0 Hz, 1P), 22.8 (d, *J* = 185.2, 69.6, Hz, 1P). FAB MS: *m/z* 1049 (M$^+$).

[Ru$_3$(CO)$_6$(PPh$_3$)(μ-dppm)(μ$_3$-η^2-C$_4$H$_2$S){μ-P(C$_4$H$_3$S)$_2$}(μ-H)] (8). PPh$_3$ (12 mg, 0.046 mmol) was added to a solution of **4** (50 mg, 0.043 mmol) in 25 cm^3 of benzene. The reaction mixture

Table 1 Crystallographic data and structure refinement[a] for **2**, **4–7**, **9** and **12**

	2	**4**	**5**·CH_2Cl_2	**6**	**7**	**9**·CH_2Cl_2	**11**·1.5CH_2Cl_2
Empirical formula	$C_{46}H_{31}O_9P_3Ru_3S_3$	$C_{44}H_{31}O_7P_3Ru_3S_3$	$C_{44}H_{33}Cl_2O_6P_3Ru_3S_3$	$C_{44}H_{31}O_{10}P_3Ru_3$	$C_{40}H_{27}O_9P_3Ru_3$	$C_{62}H_{48}Cl_2O_9P_4Ru_3$	$C_{44}H_{31}Br_2Cl_3O_9P_3Ru_3$
M_r	1220.01	1162.98	1220.90	1115.81	1047.74	1434.99	1365.98
Crystal system	Monoclinic	Monoclinic	Monoclinic	Triclinic	Monoclinic	Monoclinic	Monoclinic
Space group	$C2/c$	$P2_1/c$	$P2_1/n$	$P\bar{1}$	$P2_1/c$	$P2_1/c$	$P2_1/n$
a/Å	40.633(2)	12.0040(7)	10.385(3)	10.0968(6)	18.181(2)	12.6863(12)	18.4093(14)
b/Å	11.3727(6)	33.7698(19)	22.461(6)	11.7495(7)	11.2861(12)	24.922(2)	11.1295(9)
c/Å	19.9649(11)	11.4887(7)	19.081(6)	19.6334(12)	19.761(2)	20.944(2)	25.182(2)
α/°	90	90	90	79.8620(10)	90	90	90
β/°	92.0600(10)	110.2400(10)	93.835(5)	75.9750(10)	102.168(2)	99.356(2)	109.2910(10)
γ/°	90	90	90	67.8240(10)	90	90	90
V/Å^3	9220.0(9)	4369.6(4)	4441(2)	2083.3(2)	3963.8(7)	6533.8(11)	4869.8(7)
Z	8	4	4	2	4	4	4
D_c/g cm^{-3}	1.758	1.768	1.826	1.779	1.756	1.459	1.863
μ (Mo Kα)/mm^{-1}	1.266	1.327	1.425	1.248	1.304	0.915	2.875
F(000)	4832	2300	2416	1104	2064	2872	2660
Crystal size/mm	0.45 × 0.12 × 0.03	0.12 × 0.10 × 0.08	0.26 × 0.21 × 0.15	0.46 × 0.42 × 0.15	0.46 × 0.24 × 0.06	0.48 × 0.12 × 0.06	0.28 × 0.24 × 0.06
θ range/Å	1.00 to 28.30	1.91 to 28.28	2.47 to 28.28	2.65 to 28.30	2.77 to 28.29	1.94 to 28.36	2.52 to 28.30
Index ranges	$-51 \leq h \leq 52$ $-14 \leq k \leq 14$ $-25 \leq l \leq 25$	$-15 \leq h \leq 14$ $-44 \leq k \leq 44$ $-15 \leq l \leq 13$	$-13 \leq h \leq 13$ $-29 \leq k \leq 29$ $-24 \leq l \leq 25$	$-12 \leq h \leq 13$ $-15 \leq k \leq 15$ $-25 \leq l \leq 26$	$-23 \leq h \leq 24$ $-14 \leq k \leq 14$ $-25 \leq l \leq 25$	$-16 \leq h \leq 16$ $-32 \leq k \leq 32$ $-27 \leq l \leq 27$	$-23 \leq h \leq 23$ $-14 \leq k \leq 14$ $-32 \leq l \leq 33$
Reflections collected	39753	25607	37786	17922	33672	54742	41071
Independent reflections	10913 [R(int) = 0.0379]	10148 [R(int) = 0.0246]	10587 [R(int) = 0.0486]	9527 [R(int) = 0.0210]	9487 [R(int) = 0.0345]	15378 [R(int) = 0.0812]	11631 [R(int) = 0.0450]
Max. and min. trans	0.5997 and 0.9630	0.8570 and 0.9013	0.7082 and 0.8146	0.8349 and 0.5975	0.9259 and 0.5854	0.9471 and 0.6677	0.8464 and 0.4999
Data/restraints/parameters	10913/0/567	10148/0/531	10587/0/550	9527/0/545	9487/0/496	15378/0/764	11631/0/590
Goodness-of-fit on F^2	1.021	1.013	1.056	1.042	1.025	1.074	1.010
Final R indices [$I > 2\sigma(I)$]	$R_1 = 0.0337$ $wR_2 = 0.0750$	$R_1 = 0.0326$ $wR_2 = 0.0747$	$R_1 = 0.0386$ $wR_2 = 0.0931$	$R_1 = 0.0306$ $wR_2 = 0.0856$	$R_1 = 0.0290$ $wR_2 = 0.0687$	$R_1 = 0.0814$ $wR_2 = 0.1997$	$R_1 = 0.0442$ $wR_2 = 0.1082$
R indices (all data)	$R_1 = 0.0454$ $wR_2 = 0.0791$	$R_1 = 0.0404$ $wR_2 = 0.0776$	$R_1 = 0.0491$ $wR_2 = 0.0971$	$R_1 = 0.0347$ $wR_2 = 0.0890$	$R_1 = 0.0342$ $wR_2 = 0.0707$	$R_1 = 0.1109$ $wR_2 = 0.2150$	$R_1 = 0.0591$ $wR_2 = 0.1159$
Largest diff peak and hole/e Å^{-3}	1.198 and −1.383	1.385 and −0.821	2.056 and −0.623	1.014 and −0.589	0.900 and −0.719	2.672 and −1.060	1.351 and −1.439

[a] Details in common: Mo-Kα (λ = 0.71073 Å), temperature (K) 150(2), refinement method: full-matrix least-squares on F^2.

was heated to reflux for 3 h. After the mixture was cooled, the solvent was removed in *vacuo.* The product was separated by TLC using a 7:3 hexane/CH_2Cl_2 solvent mixture to yield $[Ru_3(CO)_6(PPh_3)(\mu\text{-dppm})(\mu_3\text{-}\eta^2\text{-}C_4H_2S)\{\mu\text{-}P(C_4H_3S)_2\}(\mu\text{-}H)]$ (**8**) (30 mg, 73%) as yellow crystals from hexane/CH_2Cl_2 at 4°C. Calc. for $C_{61}H_{46}O_6P_4Ru_3S_3$: C, 52.40; H, 3.32. Found: C, 52.69; H, 3.47. IR (νCO, CH_2Cl_2) 2057 w, 2015 *vs*, 1973 s, 1954 s cm^{-1}. ^1H NMR ($CDCl_3$): major isomer (**8a**) δ 7.81 (m, 2H), 7.57 (m, 6H), 7.44 (m, 4H), 7.35 (m, 20H), 7.16 (m, 6H), 7.01 (m, 2H), 6.87 (m, 1H), 6.65 (m, 1H), 6.09 (m, 1H), 4.01 (m, 1H), 2.60 (m, 1H), –14.36 (m, 1H). $^{31}P\{^1H\}$ NMR ($CDCl_3$): major isomer (**8a**) δ 50.1 (m, 1P), 40.8 (m, 1P), 32.8 (m, 1P), 9.9 (m, 1P); ^1H NMR ($CDCl_3$): minor isomer (**8b**) δ 7.78 (m, 2H), 7.66 (m, 6H), 7.47 (m, 4H), 7.22 (m, 20H), 7.11 (m, 6H), 6.92 (m, 2H), 6.57 (m, 1H), 6.31 (m, 1H), 6.19 (m, 1H), 3.51 (m, 1H), 2.80 (m, 1H), –14.55 (m, 1H). $^{31}P\{^1H\}$ NMR ($CDCl_3$): minor isomer (**8b**) δ 47.5 (m, 1P), 37.0 (m, 1P), 31.9 (m, 1P), 8.7 (m, 1P). FAB MS: *m*/*z* 1399 (M^+).

$[Ru_3(CO)_6(PPh_3)(\mu\text{-dppm})(\mu_3\text{-}\eta^2\text{-}C_4H_2O)\{\mu\text{-}P(C_4H_3O)_2\}(\mu\text{-}H)]$ (9). A similar reaction to that above using **6** (60 mg, 0.054 mmol) and PPh_3 (15 mg, 0.057 mmol) in benzene (25 cm^3) followed by similar work-up and chromatographic separation afforded $[Ru_3(CO)_6(PPh_3)(\mu\text{-dppm})(\mu_3\text{-}\eta^2\text{-}C_4H_2O)\{\mu\text{-}P(C_4H_3O)_2\}(\mu\text{-}H)]$ (**9**) (50 mg, 68%) as yellow crystals after recrystallisation from hexane/CH_2Cl_2 at 4 °C. Calc. for $C_{61}H_{46}O_9P_4Ru_3$: C, 54.27; H, 3.43. Found: C, 54.42; H, 3.67. IR (νCO, CH_2Cl_2) 2031 w, 2014 *vs*, 1974 s, 1956 s cm^{-1}. ^1H NMR ($CDCl_3$): major isomer (**9a**) δ 7.56 (m, 5H), 7.12 (m, 25H), 6.84 (m, 4H), 6.67 (m, 3H), 6.38 (m, 2H), 6.15 (m, 1H), 5.96 (m, 2H), 5.57 (m, 1H), 3.42 (m, 1H), 2.65 (m, 1H), –14.76 (m, 1H). $^{31}P\{^1H\}$ NMR ($CDCl_3$): major isomer (**9a**) δ 50.3 (m, 1P), 40.7 (m, 1P), 35.8 (m, 1P), –0.1 (m, 1P). ^1H NMR ($CDCl_3$): maior isomer (**9b**) δ 7.76 (m, 4H), 7.38 (m, 4H), 7.21 (m, 25H), 6.94 (m, 3H), 6.89 (m, 2H), 6.42 (m, 2H) 6.20 (m, 1H), 5.87 (m, 1H), 5.64 (m, 1H), 3.20 (m, 1H), 2.76 (m, 1H), –15.0 (m, 1H). $^{31}P\{^1H\}$ NMR ($CDCl_3$): minor isomer (**9b**) δ 50.2 (m, 1P), 38.1 (m, 1P), 33.4 (m, 1P), –1.1 (m, 1P). FAB MS: *m*/*z* 1351 (M^+).

$[Ru_3(CO)_6Br(\mu\text{-}Br)(\mu\text{-dppm})(\mu_3\text{-}\eta^2\text{-}C_4H_2S)\{\mu\text{-}P(C_4H_3S)_2\}(\mu\text{-}H)]$ (10). Hydrogen bromide gas was bubbled through a THF solution (12 cm^3) of **4** (20 mg, 0.017 mmol) for 1 min. and immediately the color changed from pale yellow to yellow. Analytical TLC indicated complete consumption of **4** and formation of a single product. Removal of solvent under reduced pressure and chromatographic separation of the residue on silica TLC plates eluting with hexane/CH_2Cl_2 gave $[Ru_3(CO)_6Br(\mu\text{-}Br)(\mu\text{-dppm})(\mu_3\text{-}\eta^2\text{-}C_4H_2S)\{\mu\text{-}P(C_4H_3S)_2\}(\mu\text{-}H)]$ (**10**) (13 mg, 58%) as yellow crystals after recrystallisation from hexane/$CHCl_3$ at by slow evaporation of the solvents. Calc. for $C_{43}H_{31}Br_2O_6P_3Ru_3S_3$: C, 39.86; H, 2.41. Found: C, 40.22; H, 2.59. IR (νCO, CH_2Cl_2) 2027 w, 2015 *vs*, 1971 s, 1956 s cm^{-1}. ^1H NMR ($CDCl_3$): δ 8.62 (s, 1H), 7.98 (s, 1H), 7.82 (m, 3H), 7.71–7.54 (m, 13H), 7.39–7.27 (m, 6H), 6.96 (s, 1H) 6.70 (s, 1H), 6.59 (s, 2H), 4.84 (m, 1H), 2.95 (m, 1H), –11.87 (dd, J = 13.4, 9.6 Hz, 1H). $^{31}P\{^1H\}$ NMR ($CDCl_3$): δ 48.4 (d, J = 70.4 Hz, 1P), 21.7 (dd, J = 70.4, 91.6 Hz, 1P), –9.8 (d, J = 91.6 Hz, 1P). MS (FAB): *m*/*z* 1297 (M^+).

$[Ru_3(CO)_6Br(\mu\text{-}Br)(\mu\text{-dppm})(\mu_3\text{-}\eta^2\text{-}C_4H_2O)\{\mu\text{-}P(C_4H_3O)_2\}(\mu\text{-}H)]$ (11). A similar reaction to that above of **6** (15 mg, 0.014 mmol) with HBr followed by similar chromatographic separation afforded $[Ru_3(CO)_6Br(\mu\text{-}Br)(\mu\text{-dppm})(\mu_3\text{-}\eta^2\text{-}C_4H_2O)\{\mu\text{-}P(C_4H_3O)_2\}(\mu\text{-}H)]$ (**11**) (9 mg, 51%) as yellow crystals after recrystallisation from hexane/$CHCl_3$ at 25 °C. Calc. for $C_{43}H_{31}Br_2O_9P_3Ru_3$: C, 41.39; H, 2.50. Found: C, 41.62; H, 2.76. IR (νCO, CH_2Cl_2) 2031 w, 2014 *vs*, 1974 s, 1956 s cm^{-1}. ^1H NMR ($CDCl_3$): δ 8.57 (s, 1H), 7.44 (s, 1H), 7.60 (m, 3H), 7.54–7.32 (m, 13H), 7.16–7.01 (m, 6H), 6.66 (s, 1H) 6.50 (s, 1H), 6.35 (s, 1H), 4.45 (m, 1H), 3.71 (s, 1H), 2.95 (m, 1H), –11.85 (dd, J = 12.8, 8.8 Hz, 1H). $^{31}P\{^1H\}$ NMR ($CDCl_3$): δ 48.3 (d, J = 64.4 Hz, 1P), 22.1 (dd, J = 85.6, 64.4 Hz, 1P), –10.10 (d, J = 85.6 Hz, 1P). MS (FAB): *m*/*z* 1249 (M^+).

Crystallography†

Single crystals of **2**, **4–7**, **9** and **11** suitable for X-ray diffraction were grown by slow diffusion of hexane into a dichloromethane solution at 4 °C. All geometric and crystallographic data **2**, **4–7**, **9** and **11** were collected at 150 K on a Bruker SMART APEX CCD diffractometer using Mo-Kα radiation (λ = 0.71073 Å). Data reduction and integration was carried out with SAINT+ and absorption corrections were applied using the program SADABS.[48] Structures were solved by direct methods and developed using alternating cycles of least-squares refinement and difference-Fourier synthesis. All non-hydrogen atoms were refined anisotropically. Hydrogen atoms were placed in the calculated positions and their thermal parameters linked to those of the atoms to which they were attached (riding model). The SHELXTL PLUS V6.10 program package was used for structure solution and refinement.[49] Final difference maps did not show any residual electron density of stereochemical significance. The details of the data collection and structure refinement are given in Table 1.

Acknowledgements

M.N.U. thanks Hajee Mohammad Danesh Science and Technology University for study leave to work at Jahangirnagar University. S.E.K. acknowledges The Royal Society (London) for a fellowship to work at University College London and Jahangirnagar University for sabbatical leave. N.B. thanks Sher-e-Bangla Agricultural University for leave to work at Lund University. This research has been sponsored by the Swedish International Development Agency (SIDA) *via* the *Swedish Research Links* programme and the Swedish Research Council (VR).

References

1 R. J. Angelici, *Polyhedron*, 1997, **16**, 3073.
2 R. J. Angelici, *Coord. Chem. Rev.*, 1990, **105**, 61.
3 C. Bianchini and A. Meli, *J. Chem. Soc., Dalton Trans.*, 1996, 801.
4 T. B. Rauchfuss, *Prog. Inorg. Chem.*, 1991, **21**, 259.
5 M. A. Reynolds, I. A. Guzei and R. J. Angelici, *Organometallics*, 2001, **20**, 1071.
6 A. J. Deeming, M. K. Shinhmar, A. J. Arce and Y. De Sanctis, *J. Chem. Soc., Dalton Trans.*, 1999, 1153.
7 A. J. Deeming, S. N. Jayasuria, A. J. Arce and Y. De Sanctis, *Organometallics*, 1996, **15**, 786.
8 J. D. King, M. Monari and E. Nordlander, *J. Organomet. Chem.*, 1999, **573**, 272.
9 N. K. K. Kazemifar, M. J. Stchedroff, M. A. Mottalib, S. Selva, M. Monari and E. Nordlander, *Eur. J. Inorg. Chem.*, 2006, 2058.
10 S. P. Tunik, I. O. Koshevoy, A. J. Poë, D. H. Farrar, E. Nordlander, M. Haukka and T. A. Pakkanen, *Dalton Trans.*, 2003, 2457.

11 K. Bieger, F. Estevan, P. Lahuerta, P. Hirva, J. Perez-Prieto, M. Sanau, N. Siguero and S.-E. Stiriba, *Organometallics*, 2003, **22**, 1799.

12 F. Estevan, P. Lahuerta, J. Lloret, J. Perez-Prieto and M. Sanau, *Organometallics*, 2006, **25**, 3156.

13 M. A. Mottalib, S. E. Kabir, D. A. Tocher, A. J. Deeming and E. Nordlander, *J. Organomet. Chem.*, 2007, **692**, 5007.

14 U. Bodensieck, H. Vahrenkamp, G. Rheinwald and H. Stoeckli-Evans, *J. Organomet. Chem.*, 1995, **488**, 85.

15 N. Begum, M. A. Rahman, M. R. Hassan, D. A. Tocher, E. Nordlander, G. Hogarth and S. E. Kabir, *J. Organomet. Chem.*, 2008, **693**, 1645.

16 M. A. Mottalib, S. E. Kabir, D. A. Tocher, A. J. Deeming and E. Nordlander, *J. Organomet. Chem.*, 2007, **692**, 5007.

17 M. Ackermann, A. Pascarifu, T. Höcher, H.-U. Siehl and S. Berger, *J. Am. Chem. Soc.*, 2006, **128**, 8434.

18 W.-Y. Wong, F.-L. Ting and W.-L. Lam, *J. Chem. Soc., Dalton Trans.*, 2001, 2981.

19 W.-Y. Wong, F.-L. Ting and Z. Lin, *Organometallics*, 2003, **22**, 5100.

20 F. A. Cotton and B. E. Hanson, *Inorg. Chem.*, 1977, **16**, 3369.

21 S. E. Kabir and G. Hogarth, *Coord. Chem. Rev.*, 10.1016/j.ccr.2008.08.013.

22 N. Lugan, J. J. Bonnet and J. A. Ibers, *J. Am. Chem. Soc.*, 1985, **107**, 4484.

23 M. I. Bruce, P. A. Humphrey, B. W. Skelton, A. H. White and M. L. Williams, *Aust. J. Chem.*, 1985, **38**, 1301; M. I. Bruce, O. Bin Shawkataly and M. L. Williams, *J. Organomet. Chem.*, 1985, **287**, 127.

24 A. A. Torabi, A. S. Humphreys, G. A. Koutsantonis, B. W. Skelton and A. H. White, *J. Organomet. Chem.*, 2002, **655**, 227.

25 C. J. Adams, M. I. Bruce, O. Kühl, B. W. Skelton and A. H. White, *J. Organomet. Chem.*, 1993, **445**, C6.

26 Md. I. Hyder, S. E. Kabir, Md. A. Miah, T. A. Siddique and G. M. G. Hossain, *Polyhedron*, 2005, **24**, 1471.

27 F. Van Gastel, J. F. Corrigan, S. Doherty, N. J. Taylor and A. J. Carty, *Inorg. Chem.*, 1992, **31**, 4492.

28 S. A. McLaughlin, N. J. Taylor and A. J. Carty, *Can. J. Chem.*, 1982, **60**, 87.

29 A. J. Deeming, A. J. Arce, Y. De Sanctis, M. W. Day and K. I. Hardcastle, *Organometallics*, 1890, **8**, 1408.

30 W. Coleman, D. F. Jones, P. H. Dixneuf, C. Brission, J. J. Bonnet and G. Lavigne, *Inorg. Chem.*, 1984, **23**, 952.

31 M. I. Bruce, M. J. Liddell and B. K. Nicholson, *Appl. Organomet. Chem.*, 1990, **4**, 457.

32 P. R. Raithby and M. J. Rosales, *Adv. Inorg. Chem. Radiochem.*, 1985, **29**, 169.

33 E. El Amin, J. C. Jeffery and T. M. Walters, *J. Chem. Soc., Chem. Commun.*, 1990, 170; S. A. Brew, S. J. Dossett, J. C. Jeffery and F. G. A. Stone, *J. Chem. Soc., Dalton Trans.*, 1990, 3709.

34 E. Cabrera, J. C. Daran, Y. Jeannin and O. Kristiansson, *J. Organomet. Chem.*, 1986, **310**, 367.

35 F. Muller, G. van Koten, M. J. Kraakman, K. Vrees, D. Heijdenrijk and M. C. Zoutberg, *Organometallics*, 1989, **8**, 1331.

36 R. D. Adams and J. T. Tanner, *Organometallics*, 1988, **7**, 2241.

37 R. D. Adams, G. Chen, S. Sun, J. T. Tanner and T. A. Wolfe, *Organometallics*, 1990, **9**, 251.

38 A. J. Deeming, S. E. Kabir, D. Nuel and N. I. Powell, *Organometallics*, 1989, **8**, 717.

39 J. Louie and R. H. Grubbs, *Organometallics*, 2002, **21**, 2153.

40 S. E. Kabir L. Salassa, and G. Hogarth, *unpublished results*.

41 M. G. Karpov, S. P. Tunik, V. R. Denisov, G. L. Starova, A. B. Nikol'skii, F. M. Dolgushin, A. I. Yanovsky and Y. T. Struchkov, *J. Organomet. Chem.*, 1995, **485**, 219.

42 A. J. Edwards, M. A. Gallop, B. F. G. Johnson, J. U. Köhler, J. Lewis and P. R. Raithby, *Angew. Chem., Int. Ed. Engl.*, 1994, **33**, 1093.

43 S. P. Tunik, I. A. Balova, M. E. Borovitov, E. Nordlander, M. Haukka and T. A. Pakkanen, *J. Chem. Soc., Dalton Trans.*, 2002, 827.

44 A. J. Edwards, J. U. Köhler, J. Lewis and P. R. Raithby, *J. Chem. Soc., Dalton Trans.*, 1995, 3251.

45 J. U. Köhler, J. Lewis and P. R. Raithby, *Angew. Chem., Int. Ed. Engl.*, 1996, **35**, 993.

46 J. U. Köhler, J. Lewis, P. R. Raithby and A. M. Rennie, *Organometallics*, 1997, **16**, 3851.

47 M. I. Bruce, B. K. Nicholson and M. L. Williams, *Inorg. Synth.*, 1990, **26**, 265.

48 *SMART and SAINT software for CCD diffractometers*, version 6.1, Madison, WI, 2000.

49 G. M. Sheldrick, *SHELXTL PLUS*, version 6.1, Bruker AXS, Madison, WI, 2000.